Canadian Mineralogist
Vol. 14, pp. 143-148 (1976)

A REFINEMENT OF THE CRYSTAL STRUCTURE OF ADAMITE

F. C. HAWTHORNE
Dept. of Earth Sciences, University of Manitoba, Winnipeg

ABSTRACT

Three-dimensional counter-diffractometer X-ray data and a full-matrix least-squares method have been used to refine the crystal structure of adamite (Zn_2AsO_4OH; *a* 8.304(2), *b* 8.530(2), *c* 6.047(1)Å, $Z = 4$) in the space-group *Pnnm*. The final *R*-factor for 613 reflections is 4.4%.

Edge-sharing chains of $ZnO_4(OH)_2$ octahedra extend parallel to the *c*-axis, and are linked by As tetrahedra to form channels parallel to *c*. Pairs of edge-sharing ZnO_4OH trigonal dipyramids occur in these channels. The structure is similar to that of andalusite. Both bond-strength considerations and the infrared spectrum indicate the presence of weak hydrogen bonding.

SOMMAIRE

Les données tridimensionnelles obtenues par diffraction des rayons X sur diffractomètre à compteur ainsi que la méthode des moindres carrés à mattrice complète ont été utilisées pour affiner la structure cristalline de l'adamine (Zn_2AsO_4OH; *a* 8.304(2), *b* 8.530(2), *c* 6.047(1)Å, $Z = 4$) dans le groupe spatial *Pnnm*. Le résidu final pour les 613 réflexions est $R = 4.4\%$.

Des chaînes d'octaèdres $ZnO_4(OH)_2$ à arêtes communes sont alignées parallèlement à l'axe *c* et liées entre elles par des tétraèdres As de façon à former des canaux parallèles à *c*. Des paires de dipyramides trigonales ZnO_4OH à arêtes communes occupent ces canaux. La structure est semblable à celle de l'andalousite. Les valences de liaison et le spectre infrarouge indiquent la présence de ponts hydrogène faibles.

(Traduit par le journal)

INTRODUCTION

Adamite, Zn_2AsO_4OH, is a supergene mineral which occurs in the oxidation zone of zinc-bearing ore deposits. Its structure was solved by Kokkoros (1938) who showed that it was similar to that of andalusite (Al_2SiO_4O), as proposed by Strunz (1937). However, unlike andalusite, the tetrahedral part of the structure appeared to be extremely distorted with the As-O bonds varying between 1.59 and 1.81Å in length. Such large distortions are unknown in arsenates containing isolated tetrahedral AsO_4^{3-} groups, and as part of a study on the stereochemistry of the $M^{5+}O_4^{3-}$ groups, the structure of adamite was refined in order to see if such large distortions actually do occur.

EXPERIMENTAL

The crystals used in this study were from Durango, Mexico. As there was very little material available, only a partial chemical analysis could be performed; the results are given in Table 1. Normalization to two non-tetrahedral cations, together with the final <As-O> distance obtained, indicates that the adamite used in this study closely approaches the ideal stoichiometric composition, $Zn_2AsO_4(OH)$.

TABLE 1. MISCELLANEOUS INFORMATION

ZnO=56.59, CuO=0.02, FeO=0.01 wt.%, MnO not detected
formula unit $Zn_2AsO_4(OH)$

a	8.304(2)Å	μ(cm^{-1})	195
b	8.530(2)	Crystal Size (mm)	0.25
c	6.047(1)	Rad/Mono.	Mo/C
V	428.3Å^3	Total no. of $\lvert F_{obs}\rvert$	782
Space Group	*Pnnm*	No. of $\lvert F_{obs}\rvert > 4\sigma$	613
Z	4	Final *R* (observed data)	4.4%
D_{calc}	4.444	Final R_w (observed data)	4.9%

$R = \Sigma(|F_{obs}| - |F_{calc}|) / \Sigma|F_{obs}|$

$R_w = \left[\Sigma\, w(|F_{obs}| - |F_{calc}|)^2 / \Sigma\, wF_{obs}^2\right]^{\frac{1}{2}}$, w=1

Temperature factor form used: $\exp -\left[\sum_{i=1}^{3}\sum_{j=1}^{3} h_i h_j \beta_{ij}\right]$

Single-crystal precession photographs exhibited orthorhombic symmetry with systematic absences *h*0*l*, $h+l=2n+1$; 0*kl*, $k+l=2n+1$; *h*00, $h=2n+1$; 0*k*0, $k=2n+1$; 00*l*, $l=2n+1$. This is compatible with the space group *Pnnm* as found by Kokkoros (1938), and this was satisfactory for the refinement of the structure. Cell dimensions were determined by least-squares refinement of 15 reflections aligned automatically on a four-circle diffractometer and are presented in Table 1, together with other information per-

TABLE 2. ATOMIC POSITIONS AND ANISTROPIC TEMPERATURE FACTOR COEFFICIENTS FOR ADAMITE (β_{ij} x 10^4)

Site	Site Symmetry	x	y	z	β_{11}	β_{22}	β_{33}	β_{12}	β_{13}	β_{23}
Zn(1)	m	0.3653(2)	0.3642(2)	1/2	37(2)	44(2)	74(3)	1(2)	0	0
Zn(2)	2	1/2	0	0.2526(2)	62(2)	57(2)	65(3)	16(2)	0	0
As	m	0.2498(2)	0.2438(2)	0	32(1)	38(1)	60(2)	2(1)	0	0
0(1)	m	0.1044(10)	0.1041(10)	0	27(11)	37(11)	187(25)	-1(9)	0	0
0(2)	m	0.4237(9)	0.1478(10)	0	53(12)	53(12)	91(21)	4(10)	0	0
0(3)	1	0.2312(8)	0.3603(9)	0.2233(9)	51(9)	46(9)	75(14)	-1(9)	0	0
OH	m	0.3933(9)	0.1274(10)	1/2	31(9)	60(10)	110(19)	9(8)	-5(8)	-28(8)

TABLE 3. SELECTED INTERATOMIC DISTANCES AND ANGLES FOR ADAMITE

As-0(1)	1.696(8)Å		Zn(1)-0(1)	2.004(9)Å	
As-0(2)	1.660(8)		Zn(1)-0(1)	2.062(9)	
As-0(3)	1.684(6)	x 2	Zn(1)-0(3)	2.010(6)	x 2
			Zn(1)-OH	2.034(9)	
Mean	1.681				
			Mean	2.024	
			Zn(2)-0(2)	2.079(7)Å	x 2
			Zn(2)-0(3)	2.264(7)	x 2
			Zn(2)-OH	2.050(7)	x 2
			Mean	2.131	
As tetrahedron					
0(1)-0(2)	2.678(11)Å		0(1)-As-0(2)	105.8(3)°	
0(1)-0(3)	2.776(9)	x 2	0(1)-As-0(3)	110.4(2)	x 2
0(2)-0(3)	2.769(9)	x 2	0(2)-As-0(3)	111.8(2)	x 2
0(3)-0(3)	2.700(9)		0(3)-As-0(3)	106.6(3)	
Mean	2.745		Mean	109.5	
Zn(1) trigonal dipyramid					
0(1)-0(1)	^{s}2.482(14)Å		0(1)-Zn(1)-0(1)	75.2(3)°	
0(1)-0(3)	3.535(9)	x 2	0(1)-Zn(1)-0(3)	123.5(2)	x 2
0(1)-0(3)	2.999(8)	x 2	0(1)-Zn(1)-0(3)	94.8(2)	x 2
0(1)-OH	2.884(11)		0(1)-Zn(1)-OH	91.2(3)	
0(3)-0(3)	3.347(8)		0(3)-Zn(1)-0(3)	112.7(3)	
0(3)-OH	2.926(8)	x 2	0(3)-Zn(1)-OH	92.7(2)	x 2
Mean	3.070		Mean	100.1	
Zn(2) octahedron					
0(2)-0(2)	^{s}2.822(12)		0(2)-Zn(2)-0(2)	85.5(3)	
0(2)-0(3)	3.053(9)	x 2	0(2)-Zn(2)-0(3)	89.2(2)	x 2
0(2)-0(3)	3.235(8)	x 2	0(2)-Zn(2)-0(3)	96.2(2)	x 2
0(2)-OH	3.039(1)	x 2	0(2)-Zn(2)-OH	94.8(3)	x 2
0(3)-OH	2.842(9)	x 2	0(3)-Zn(2)-OH	82.3(2)	x 2
0(3)-OH	3.116(8)	x 2	0(3)-Zn(2)-OH	92.3(2)	x 2
OH-OH	^{s}2.804(12)		OH-Zn(2)-OH	86.3(3)	
Mean	3.016		Mean	90.1	

^{s}denotes shared edge

TABLE 4. MAGNITUDES AND ORIENTATIONS OF THE PRINCIPAL AXES OF THE THERMAL ELLIPSOIDS

	R.M.S. displacement	Angle to *a*-axis	Angle to *b*-axis	Angle to *c*-axis
Zn(1)	0.113(3)Å^2	4(9)°	94(9)°	90°
	0.117(2)	90	90	0
	0.130(3)	86(9)	4(9)	90
Zn(2)	0.110(2)	90	90	0
	0.124(3)	47(3)	137(3)	90
	0.165(3)	43(3)	47(3)	90
As	0.104(2)	15(7)	105(7)	90
	0.105(2)	90	90	0
	0.119(2)	75(7)	15(7)	90
0(1)	0.097(19)	2(46)	88(46)	90
	0.117(18)	88(46)	178(46)	90
	0.186(13)	90	90	0
0(2)	0.130(14)	90	90	0
	0.132(17)	143(66)	53(66)	90
	0.143(18)	53(66)	37(66)	90
0(3)	0.088(13)	97(14)	49(9)	41(11)
	0.127(12)	153(18)	75(15)	112(18)
	0.157(9)	116(18)	135(10)	57(11)
OH	0.103(18)	3(20)	87(2)	90
	0.143(13)	90	90	0
	0.148(15)	93(20)	3(20)	90

tinent to the data collection and refinement procedures.

The crystal used to collect the intensity data was an irregular equidimensional fragment with minimum and maximum dimensions of 0.245 and 0.265 mm respectively. It was mounted on a Syntex $P\bar{1}$ automatic diffractometer operating in the θ-2θ scan mode with variable rates from 2.0-24.0°/min. depending on the α_1-α_2 separation and the peak count through an angle of 2°, with stationary background counts at the beginning and end of each scan. Graphite monochromatized Mo$K\alpha$ radiation ($\lambda = 0.71069$Å) was used. Two standard reflections were monitored every fifty reflections to check for constancy of crystal alignment; no significant change was noted during the data collection. A total of 782 reflections was measured over one asymmetric unit out to a maximum 2θ value of 65°. Because of the near-spherical shape of the crystal, absorption was assumed to be solely a function of theta, and absorption corrections for spherical crystal shape ($\mu R = 2.5$) were performed. The data were then corrected for Lorentz, polarization and background effects and reduced to structure factors. A reflection was considered to be observed if its magnitude was greater than four standard deviations based on counting statistics; application of this criterion resulted in 613 observed reflections.

REFINEMENT

The atomic coordinates given by Kokkoros (1938) were used as initial parameters for the least-squares program RFINE (Finger 1969). Scattering factors for neutral atoms were taken from Cromer & Mann (1968) and anomalous dispersion corrections from Cromer & Lieberman (1970). The refinement converged rapidly to an R-factor (see Table 1) of 6.2% for an isotropic thermal model. The two most intense reflections (004 and 022) were significantly less than their calculated values at this stage; it was assumed that these were severely affected by extinction and they were removed from the refinement. The temperature factors were converted to anisotropic (Table 1) and a correction was made for isotropic extinction (Zachariasen 1968) with the extinction coefficient included as a variable in the refinement. Full-matrix least-squares refinement of all variables resulted in convergence at R-factors of 4.4% (observed) and 5.7% (all data), and R_w-factors of 4.9% (observed) and 5.6% (all data)*. The extinction coefficient at this stage was $0.5(3) \times 10^{-6}$; inclusion of the 004 and 022 reflections slightly increased this value and produced a slight increase in the R-factor but did not affect the positions or temperature factors. The final atomic positions and anisotropic temperature factor coefficients are presented in Table 2. Interatomic distances and angles were calculated using the program ERRORS (L. W. Finger, pers. comm.) and are given in Table 3. The magnitudes and orientations of the principal axes of the thermal ellipsoids were calculated with ERRORS and are given in Table 4.

DISCUSSION

The structure of adamite is shown in Figure 1. Arsenic is surrounded by four oxygens in a distorted tetrahedral arrangement, with the bond lengths varying between 1.66 and 1.70Å. The tetrahedral distortion is much less than that reported by Kokkoros (1938), and the range of bond lengths observed here is conformable with that displayed by most other arsenates (e.g. Poulsen & Calvo 1968; Krishnamachari & Calvo 1970, 1973; Calvo & Neelakantan 1970); extreme distortion of arsenate tetrahedra is gen-

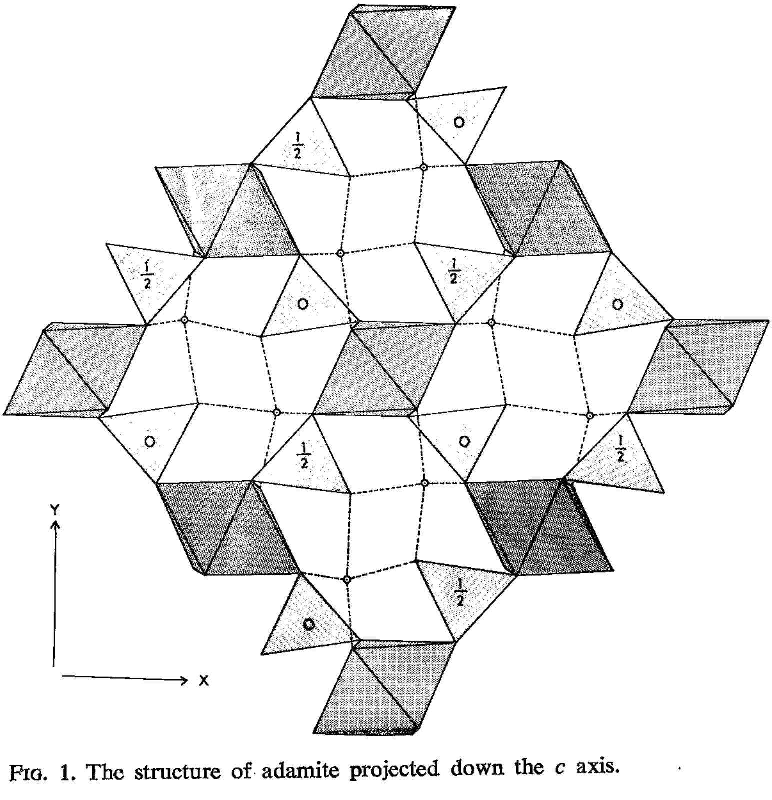

FIG. 1. The structure of adamite projected down the c axis.

---

*A list of observed and calculated structure factors has been deposited with the Depository of Unpublished Data. Copies may be obtained on request to: Depository of Unpublished Data, National Science Library, National Research Council of Canada, Ottawa, Ontario, Canada.

erally encountered only in structures containing bent pyro-groups (e.g. $Na_4As_2O_7$, Leung & Calvo 1973; $Pb_2As_2O_7$, C. Calvo, pers. comm.) and polyarsenate chains (e.g. $LiAsO_3$, Hilmer & Dornberger-Schiff 1956). Zn(1) is surrounded by four oxygen atoms and one OH group, arranged in a trigonal dipyramid. The three short equatorial bonds are statistically equal and the axial bonds are elongate; in addition, Zn(1) is slightly displaced out of the equatorial plane towards the axial OH group. Zn(2) is bonded to four oxygen atoms and two OH groups in a distorted octahedral arrangement. The octahedron is strongly elongated with Zn(2) forming long axial bonds to the O(3) oxygens, and the OH ions, which lie in the equatorial plane of the distorted octahedron, are arranged in a *cis* configuration.

Dominating the adamite structure are the chains of edge-sharing Zn(2) octahedra that extend parallel to the *c*-axis (Fig. 2), alternately sharing the O(2)-O(2) and OH-OH octahedral edges. Both the shared edge lengths and the angles subtended by them at the Zn(2) cations are contracted in agreement with Pauling's third rule (Pauling 1960). These chains are linked together by arsenate tetrahedra to form long channels parallel to the *c*-axis, as shown in Figure 1. Each channel is bounded by four chains with the octahedra occurring in layers at $z = \frac{1}{4}$ and $\frac{3}{4}$; the linking tetrahedra occur at $z = 0$ and $\frac{1}{2}$ and alternately point towards and away from the centre of the channel.

The Zn(1) atoms lie in these channels in the plane of the arsenate tetrahedra, providing linkage between the two arsenate levels at $z = 0$ and $z = \frac{1}{2}$. Zn(1) polyhedra at the same level share one edge; this edge is extremely contracted as a result of relaxation of the edge-sharing configuration to reduce the Zn(1)-Zn(1) repulsive interaction.

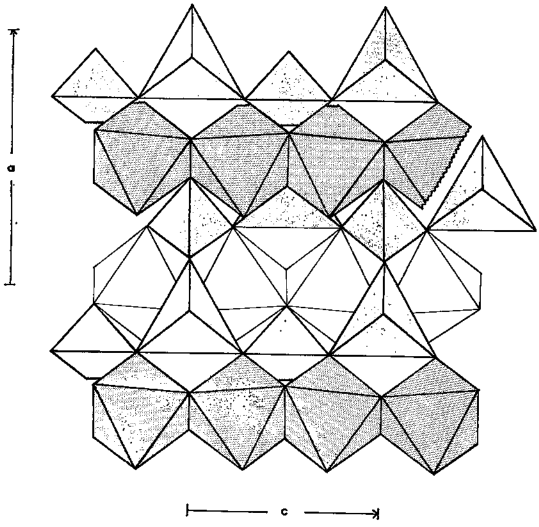

FIG. 2. Polyhedral representation of the adamite structure showing the edge-sharing octahedral chains extending parallel to *c*.

The polyhedral distortions observed in the adamite structure are similar to those found in andalusite (Burnham & Buerger 1961). In particular, the octahedron is extremely elongated in both structures. Whereas this may be due to local bond-strength considerations in andalusite (Burnham & Buerger 1961), this is not the primary reason in adamite as a formal bond-strength analysis shows net deviations of only +0.05, –0.08, +0.07 and –0.02 on O(1), O(2), OH and O(3) respectively. Examination of Figure 1 shows that a strong elongation of the axial octahedral bonds will produce a significant increase in the dimensions of the channels in the adamite structure. This will tend to offset the contraction effect of the O(1)-O(1) edge that is shared between the adjacent Zn(1) trigonal dipyramids, as this tends to reduce the size of the channel. Thus it is apparent that the long axial bonds of the octahedra are necessary for the Zn(1) dipyramid to be large enough to incorporate an atom the size of Zn.

Examination of the empirical bond-strength table for adamite (Table 5), calculated using the bond-strength curves of Brown & Shannon (1973), shows that there is a deficiency around O(3) and an excess around the OH anion. Although the discrepancies are small, they suggest the presence of hydrogen bonding between OH and O(3); using the bond-strength curves of Brown & Shannon (1973), it can be shown that an H-O(3) distance of 2.27Å produces almost ideal bond strength sums around OH and O(3). The occurrence of weak hydrogen bonding in adamite is also indicated by the infrared spectrum (Sumin de Portilla 1974). The principal OH stretching frequency occurs at 3580 cm^{-1}, slightly lower than the typical stretching frequencies (3650-3700 cm^{-1}) exhibited by OH groups not involved in hydrogen bonding.

The anisotropic thermal model appears physically reasonable, the values obtained (Table 4) falling within the range generally exhibited by well-refined crystal structures. Except for the O(3) anion, all atoms lie on special positions with one vibration direction lying parallel to the *c*-axis and the remaining two constrained to the *a*-*b* plane. In general, the principal axes of the thermal ellipsoids are oriented so as to involve the least bond stretching in their maximum vibration directions.

A large number of arsenate, vanadate, phosphate and silicate minerals have the general stoichiometry $ABXO_4(Z)$ (e.g. Richmond 1940). This group is extremely rich in both variety and complexity of structure types, many of which are as yet uncharacterized. For this reason, the present discussion will be limited to arsenates of the form $M^{2+}_2AsO_4(OH)$. Table 6 summarizes the chemical and crystallographic data available for these minerals. Adamite and its Mn-analogue eveite are isostructural whereas their dimorphs paradamite and sarkinite are not. Switzer (1956) reported an unindexed powder pattern for paradamite and suggested that it was isostructural with tarbuttite, the triclinic form of $Zn_2PO_4(OH)$; this was subsequently confirmed by Finney (1966). It was suggested by Waldrop (1970) and Moore & Smyth (1968) that sarkinite has the wagnerite structure (Coda *et al.* 1967) and this has recently been confirmed by Dal Negro *et al.* (1975).

The most apparent difference between the adamite and paradamite (tarbuttite structure, Cocco *et al.* 1966) structures is the coordination of the Zn. In adamite, one Zn atom is octahedrally coordinated by four oxygens and two hydroxyls in a *cis* arrangement, and the other Zn is coordinated by a trigonal bipyramid of four oxygens and one apical hydroxyl. In the tarbuttite-type structure, both independent Zn atoms have trigonal bipyramid coordination; one Zn is coordinated by three oxygens, one apical and one meridional hydroxyl (still a *cis* configuration) and the other Zn is coordinated by four oxygens and one meridional hydroxyl. This causes a reduction of the coordination number of one of the anions from [3] to [2]; in tarbuttite, this [2]-coordinate anion is situated close to the hydroxyl anion, suggesting that the bond-strength deficiency is compensated by hydrogen bonding. If this is the case in paradamite, the principal OH stretching frequency should be considerably lower than that exhibited by its dimorph adamite. Polyhedron polymerization is fairly similar in both structures; both have edge-sharing pairs of Zn trigonal bipyramids and isolated arsenate tetrahedra linking edge-sharing chains. However, the chains in the tarbuttite structure consist of edge-sharing trigonal bipyramids whereas the chains in the adamite structure are of edge-sharing octahedra. Despite the reduction of anion coordination number in paradamite, the polyhedral packing is more efficient, resulting in a slightly denser structure.

TABLE 5. BOND-STRENGTH TABLE FOR ADAMITE*

	Zn(1)	Zn(2)	As	Σ
O(1)	.366 .434		1.192	1.992
O(2)		$.348^{\times 2}{\rightarrow}$	1.357	2.053
OH	.397	$.379^{\times 2}{\rightarrow}$		1.173
O(3)	.427	.208	1.245	1.880
Σ	2.051	1.870	5.039	

* Calculated from the curves of Brown & Shannon (1973)

In the case of eveite and its dimorph sarkinite, far greater differences in structure exist even though the cation coordination is similar in both structures. Sarkinite has eight independent Mn atoms, half of which are in octahedral and half in trigonal bipyramidal coordination. The polymerization of the Mn octahedra is considerably more complex in sarkinite than in eveite. Three of the four octahedra share three edges with three adjacent octahedra to form a kinked infinite chain, and the fourth octahedron shares edges with two octahedra and one trigonal bipyramid. In addition, although the hydroxyls are in a *cis* arrangement, this is now an unshared edge rather than a shared edge as in eveite. Three of the four trigonal bipyramids occur in edge-sharing pairs as in eveite, while the fourth shares an edge with an octahedron. As a result of its far greater edge-sharing character, the sarkinite structure shows a far more efficient packing of the polyhedra than that exhibited by the eveite structure.

Unlike $Zn_2AsO_4(OH)$ and $Mn_2AsO_4(OH)$, $Cu_2AsO_4(OH)$ appears to exhibit only one polymorph, olivenite. Although the structure of oli-

TABLE 6. MINERALS OF THE M^{2+}_2 $AsO_4(OH)$ GROUP

NAME	Formula unit	a(Å)	b(Å)	c(Å)	(°)	(°)	(°)	Space Group
ADAMITE	$Zn_2AsO_4(OH)$	8.304(2)	8.530(2)	6.047(1)	90	90	90	Pnnm
PARADAMITE	$Zn_2AsO_4(OH)$	5.807(5)	6.666(5)	5.627(5)	104.3(1)	87.9(1)	103.2(1)	$P\bar{1}$
EVEITE	$Mn_2AsO_4(OH)$	8.57(1)	8.77(1)	6.27(1)	90	90	90	Pnnm
SARKINITE	$Mn_2AsO_4(OH)$	12.779(2)	13.596(2)	10.208(2)	90	108.9(1)	90	$P2_1/a$
OLIVENITE	$Cu_2AsO_4(OH)$	8.22	8.64	5.95	90	90	90	Pmnm(?)

venite has been solved (Heritsch 1938), some uncertainties exist concerning this structure. Heritsch (1937) originally determined the space group of olivenite as *Pmmm;* later, Heritsch (1938) solved the structure, defined the space group as *Pnnm* and indicated that the one reflection violating this symmetry was due to Renninger effects. Richmond (1940) determined the space group of olivenite as $P2_12_12_1$. Subsequently, Berry (1951) determined the space group as *Pmnm*, suggesting that the space group given by Heritsch (1937) as $D^1_{2h}(Pmmm)$ was actually a misprint for $D^{13}_{2h}(Pmnm)$. This seems not to be the case as the space group symbol appears several times in both of Heritsch's papers; in addition, the structure proposed by Heritsch (1938) is only compatible with the space group *Pnnm*. In view of the confusion existing concerning the structure of olivenite, a single crystal study is planned.

ACKNOWLEDGMENTS

The author would like to acknowledge the cooperation of the Materials Research Institute, McMaster University, Hamilton, Ontario in the collection of the *X*-ray intensity data. Financial support was provided by the National Research Council of Canada and the University of Manitoba.

REFERENCES

Berry, L. G. (1951): Observations on conichalcite, cornwallite, euchroite, liroconite and olivenite. *Amer. Mineral.* **36**, 484-503.

Brown, I. D. & Shannon, R. D. (1973): Empirical bond length — bond strength curves for oxides. *Acta Cryst.* A**29**, 266-282.

Burnham C. W. & Buerger, M. J. (1961): Refinement of the crystal structure of andalusite. *Z. Krist.* **115**, 269-290.

Calvo, C. & Neelakantan, K. (1970): Refinement of the structure of $Mg_2As_2O_7$. *Can. J. Chem.* **48**, 890-894.

Cocco, G., Fanfani, L. & Zanazzi, P. F. (1966): The crystal structure of tarbuttite. *Z. Krist.* **123**, 321-329.

Coda, A., Guiseppetti, G. & Tadini, C. (1967): The crystal structure of wagnerite. *Acc. Naz. Lincei*, Serie VIII, **43**, 211-224.

Cromer, D. T. & Mann, J. B. (1968): X-ray scattering factors computed from numerical Hartree-Fock wave functions. *Acta Cryst.* A**24**, 321-324.

——— & Lieberman, D. (1970): Relativistic calculation of anomalous scattering factors for *x*-rays. *J. Chem. Phys.* **53**, 1891-1898.

Dal Negro, A., Giuseppetti, G. & Pozas, J. M. M. (1974): The crystal structure of sarkinite, $Mn_2AsO_4(OH)$. *Tschermak's Min. Petrog. Mitt.* **21**, 246-260.

Finger, L. W. (1969): RFINE. A Fortran IV computer program for structure factor calculation and least-squares refinement of crystal structures. *Geophys. Lab., Carnegie Inst. Wash.* (unpubl.).

Finney, J. J. (1966): The unit cell of tarbuttite, $Zn_2(PO_4)(OH)$, and paradamite, $Zn_2(AsO_4)(OH)$. *Amer. Mineral.* **51**, 1218-1220.

Heritsch, H. (1937): Vorbericht uber rontgenographische Untersuchungen an Olivenit $Cu_2(OH)(AsO_4)$. *Z. Krist.* **98**, 251-353.

——— (1938): Die Struktur des Olivenites, $Cu_2(OH)(AsO_4)$. *Z. Krist.* **99**, 466-479.

Hilmer, W. & Dornberger-Schiff, K. (1956): Die Kristallstruktur von Lithium Polyarsenate $(LiAsO_3)_x$. *Acta Cryst.* **9**, 87-88.

Kokkoros, P. (1937): Uber die Struktur von Adamin. *Z. Krist.* **94**, 417-434.

Krishnamachari, N. & Calvo, C. (1970): Crystallographic studies of cobalt arsenates II. Crystal structure of $Co_8As_3O_{16}$. *Can. J. Chem.* 48, 3124-3131.

——— & ——— (1973): Magnesium arsenate, $Mg_3As_2O_8$. *Acta Cryst.* B29, 2611-2613.

Leung, K. Y. & Calvo, C. (1973): Crystal structure and phase transformations of sodium diarsenate, $Na_4As_2O_7$. *Can. J. Chem.* **51**, 2082-2088.

Moore, P. B. & Smyth, J. R. (1968): Crystal chemistry of the basic manganese arsenates: III. The crystal structure of eveite, $Mn_2(OH)(AsO_4)$. *Amer. Mineral.* **53**, 1841-1845.

Pauling, L. (1960): *The Nature of the Chemical Bond*, 3rd ed. Cornell Univ. Press, Ithaca, New York.

Poulsen, S. I. & Calvo, C. (1967): Crystal structure of $Cu_3(AsO_4)_2$. *Can J. Chem.* **46**, 917-927.

Richmond, W. E. (1940): Crystal chemistry of the phosphates, arsenates and vanadates of the type $A_2XO_4(Z)$. *Amer. Mineral.* **25**, 441-479.

Strunz, H. (1936): X-ray and morphological comparison of andalusite, libethenite and adamin. *Z. Krist.* **94A**, 60-74.

Sumin de Portilla, V. I. (1974): Infrared spectroscopic investigation of the structure of some natural arsenates and the nature of H-bonds in their structures. *Can. Min.* **12**, 262-268.

Switzer, G. (1956): Paradamite, a new zinc arsenate from Mexico. *Science* **123**, 1039.

Waldrop, L. (1970): The crystal structure of triploidite and its relation to the structures of other minerals of the triplite–triploidite group. *Z Krist.* **131**, 1-30.

Zachariasen, W. H. (1968): Extinction and Boorman effect in mosaic crystals. *Acta. Cryst.* A**28**, 421-424.

Manuscript received October 1975, emended February 1976.